Electronic Supplementary Material (ESI) for Energy & Environmental Science.

Bromide-based nonflammable electrolyte for safe and long-life sodium metal batteries

Changjian Zuo, Dejian Dong, Huwei Wang, Yue Sun, and Yi-Chun Lu*

Electrochemical Energy and Interfaces Laboratory, Department of Mechanical and Automation Engineering, The Chinese University of Hong Kong, Shatin, N.T., 999077 Hong Kong, SAR, China.

*Corresponding Author: Yi-Chun Lu. E-mail: yichunlu@mae.cuhk.edu.hk

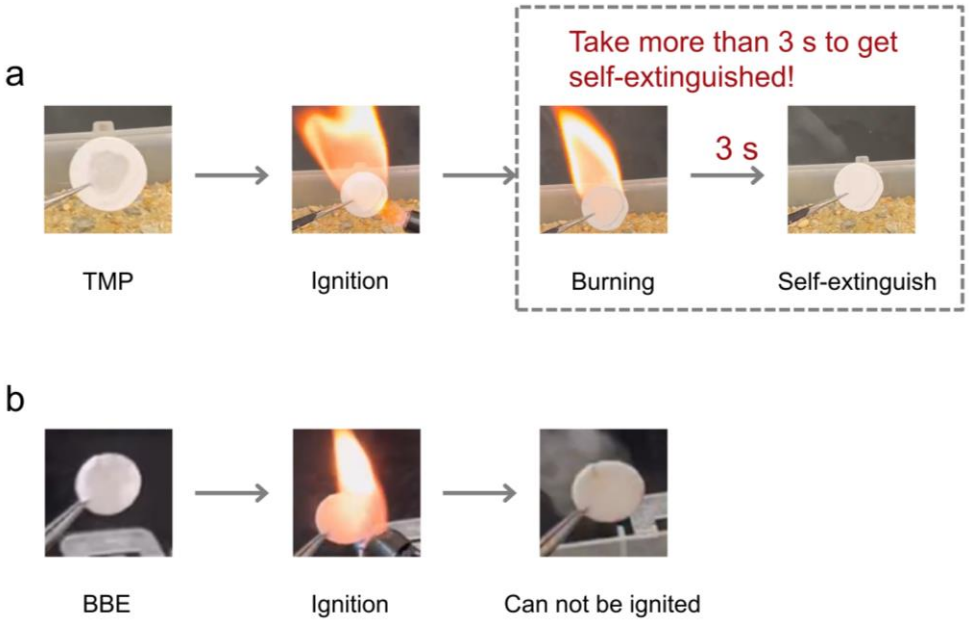

Figure S1. The digital photos of ignition experiments for TMP (a) and BBE (b) solvents.

Scavenger bonds	Bonding energy
C-Br	276 kJ/mol
C-Cl	341kJ/mol
C-F	445 kJ/mol
P-O	410 kJ/mol
P=O	544 kJ/mol

Table S1. Typical bonding energy of scavengers for the P-based, Cl-based, F-based and Br-based flame-retardants, which indicates the ability to dissociate from the retardants.

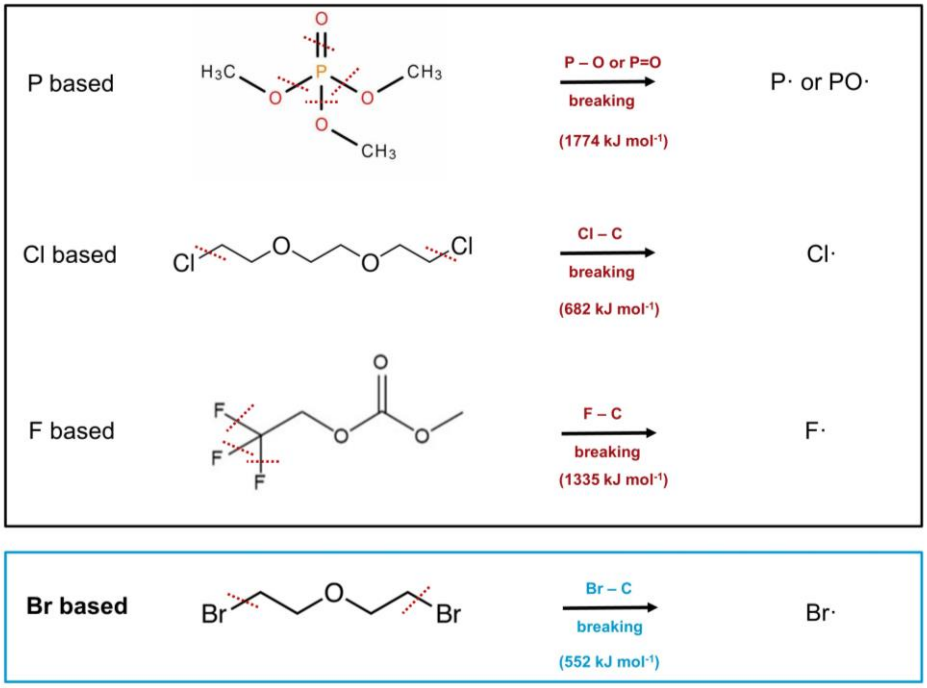

Figure S2. Dissociation processes of typical retardants when heated: the hard dissociation processes for typical P-based, Cl-based and F-based retardants in the black rectangle; the easier dissociation processes for Br-based retardant in the blue rectangle.

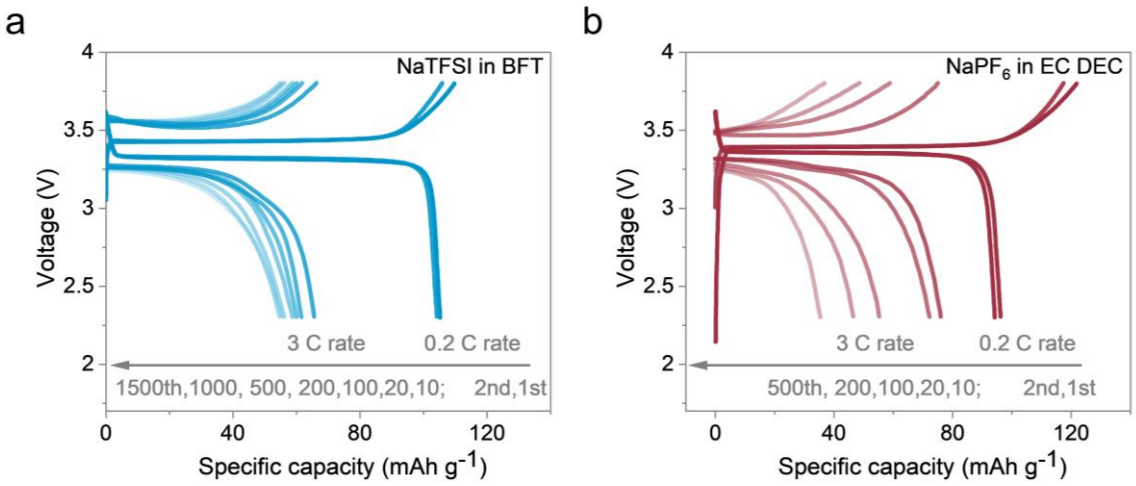

Figure S3. The cycling profiles for the $Na_3V_2(PO_4)_3$//Na cells in NaTFSI in BFT electrolyte (a) and $NaPF_6$ in EC DEC electrolyte (b).

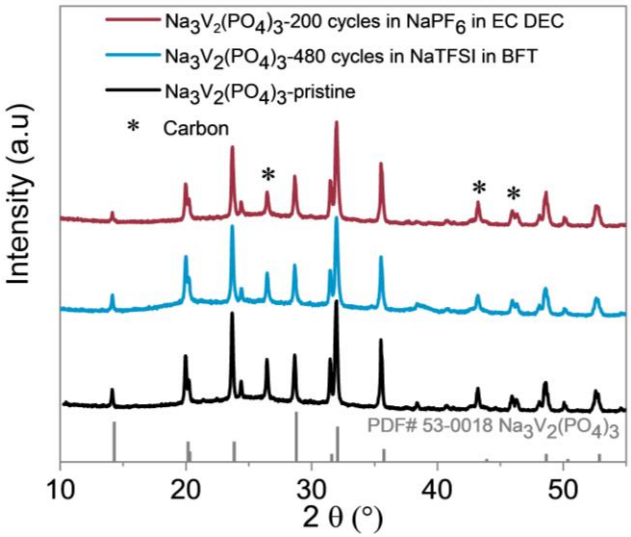

Figure S4. The XRD patterns for pristine and cycled $Na_3V_2(PO_4)_3$ cathodes in $NaPF_6$ in EC DEC electrolyte (after 200 cycles) and NaTFSI in BFT electrolyte (after 480 cycles).

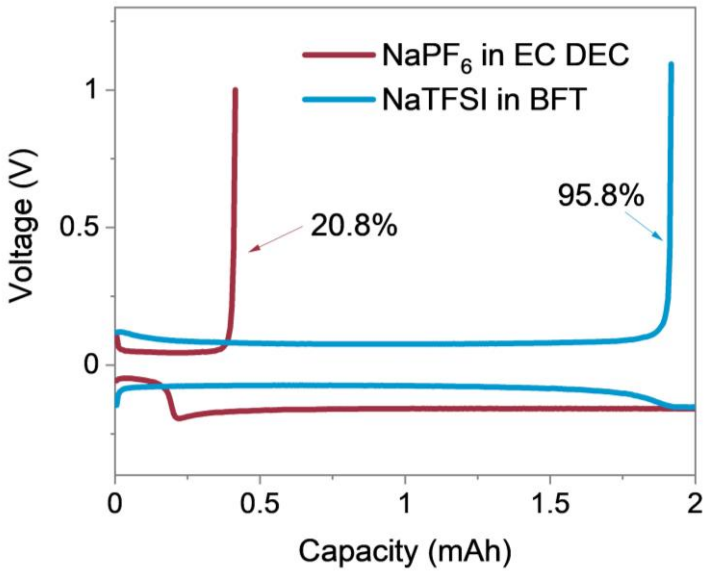

Figure S5. The coulombic efficiency plots in Na//Cu cells in $NaPF_6$ in EC DEC and NaTFSI in BFT electrolytes.

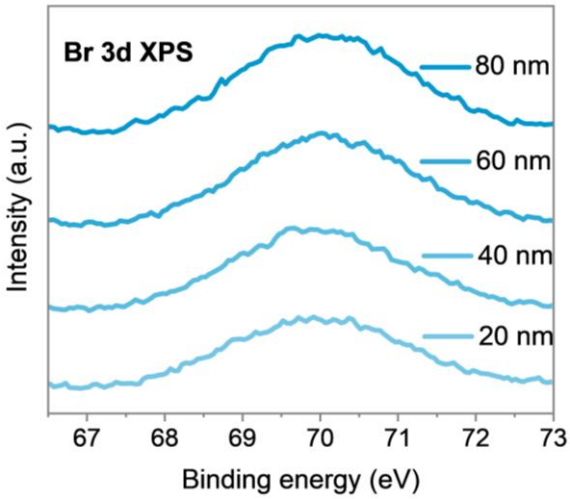

Figure S6. The Br 3d orbitals XPS spectrums at different depths sputtered by Ar^{+} of sodium anodes after cycling for 3 cycles at 0.5 mAh cm^{-2} @ 0.5 mA cm^{-2} in NaTFSI in BFT electrolyte.

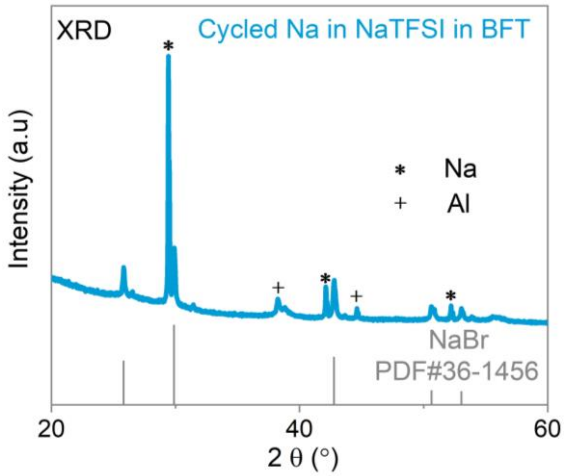

Figure S7. X-ray diffraction patterns of the cycled sodium metal anode in NaTFSI in BFT electrolyte after 3 cycles at 0.5 mAh cm^{-2} @ 0.5 mA cm^{-2}.

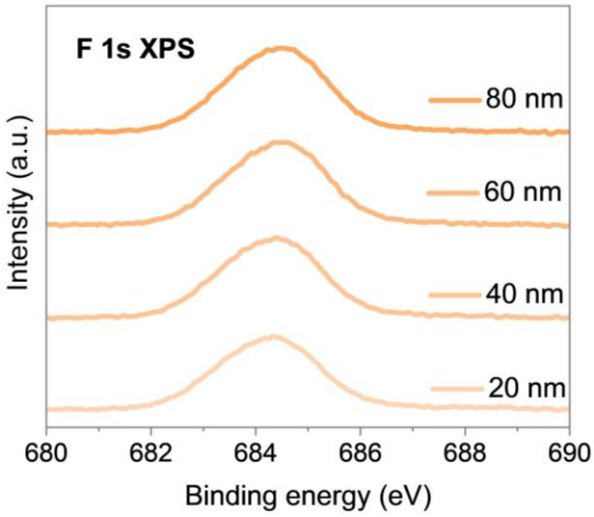

Figure S8. The F 1s orbitals XPSat different depths sputtered by Ar^{+} of sodium anodes after cycling for 3 cycles at 0.5 mAh cm^{-2} @ 0.5 mA cm^{-2} in NaTFSI in BFT electrolyte.

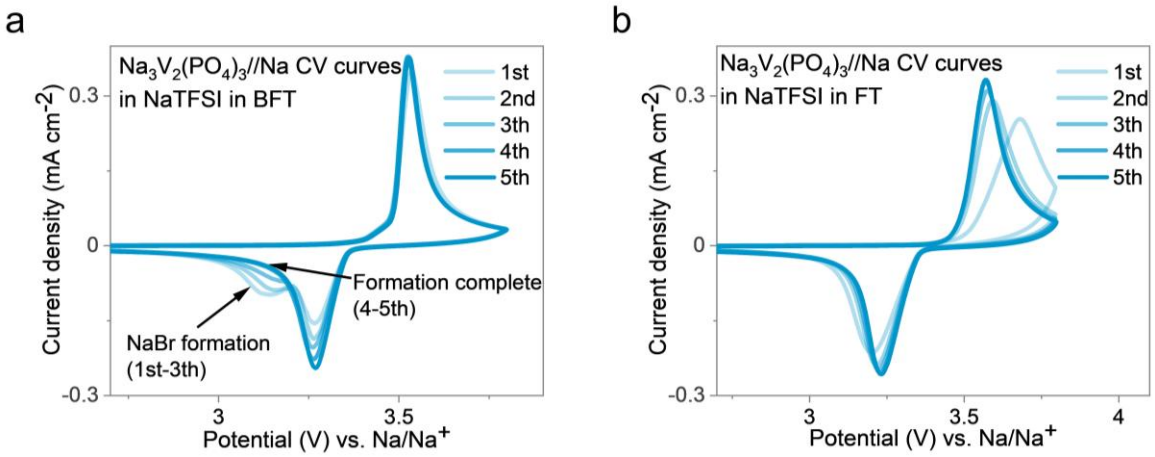

Figure S9. The CV curves from 1st-5th cycles of $Na_3V_2(PO_4)_3$//Na cells at scan rate of 0.2 mV s^{-1} between 2-3.8 V in NaTFSI in BFT electrolyte (a) and NaTFSI in FT electrolyte (b).

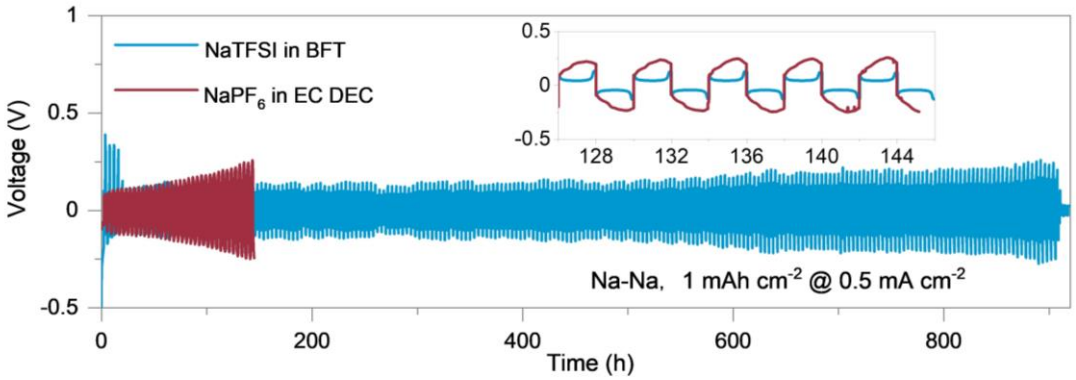

Figure S10. The Na//Na symmetric cells in NaTFSI in BFT and $NaPF_6$ in EC DEC electrolytes at 1 mAh cm^{-2} @ 0.5 mA cm^{-2}.

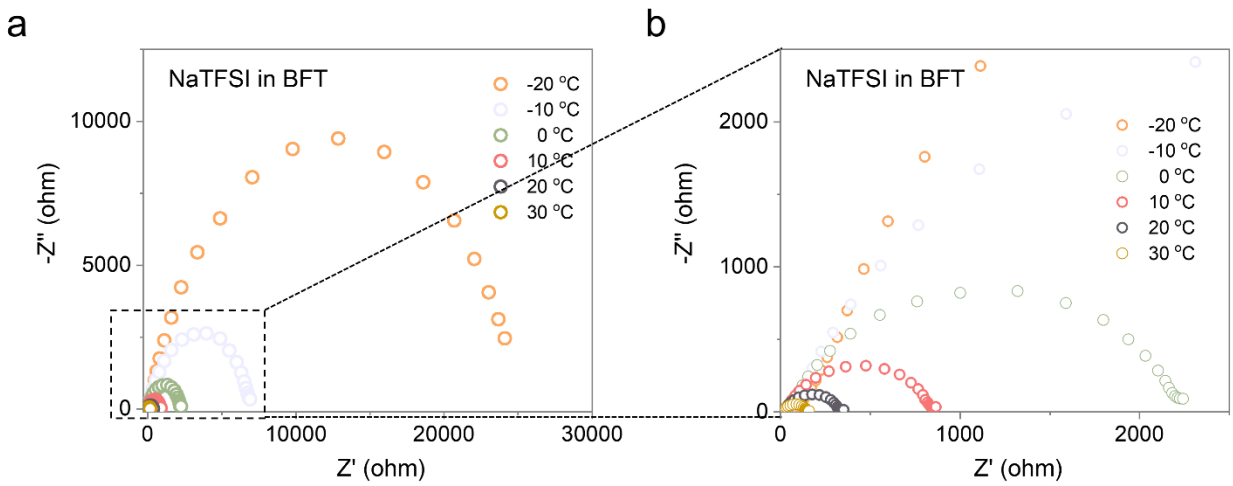

Figure S11. The EIS curves for the Na//Na symmetric cells after 3 formation cycles at 0.5 mAh cm^{-2} @ 0.5mA cm^{-2} in NaTFSI in BFT at different temperatures (a) and the enlarged patterns (b).

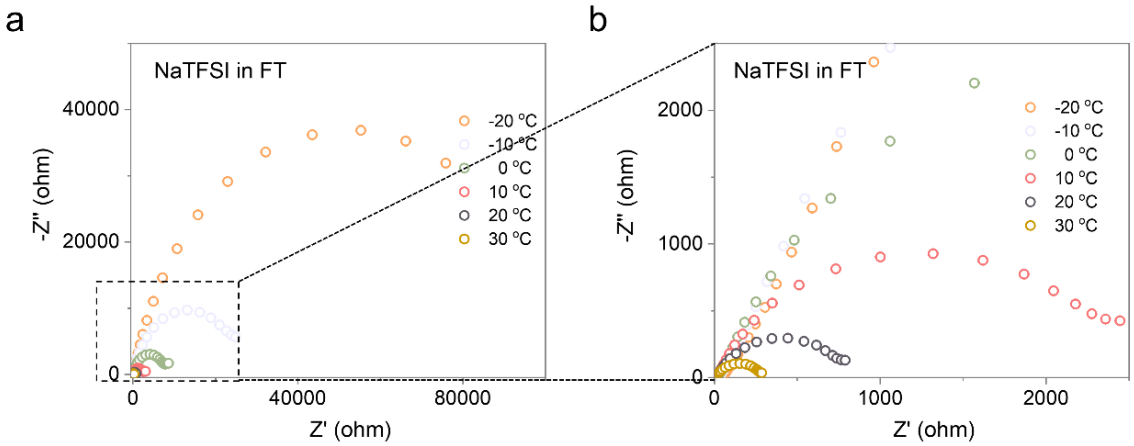

Figure S12. The EIS curves for the Na//Na symmetric cells after 3 formation cycles at 0.5 mAh cm^{-2} @ 0.5mA cm^{-2} in NaTFSI in FT at different temperatures (a) and the enlarged patterns (b).

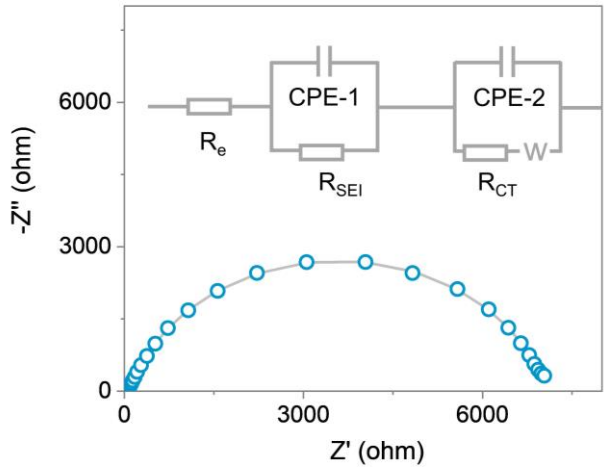

Figure S13. The circuit model used to fit the EIS curves of the symmetric cell at different temperatures. And the R_e, R_{SEI} and R_{CT} represent for the resistance of bulk electrolyte, resistance of SEI and resistance of de-solvation respectively.

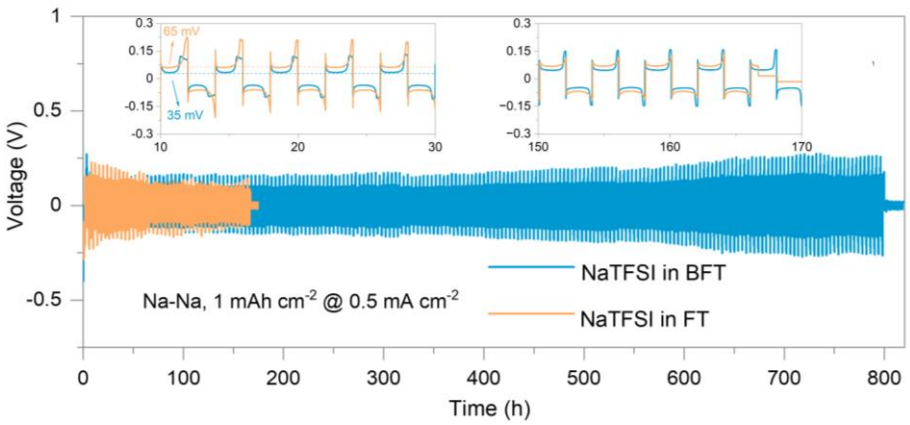

Figure S14. The Na//Na symmetric cells in NaTFSI in BFT and NaTFSI in FT electrolytes at 1 mAh cm^{-2} @ 0.5 mA cm^{-2}.

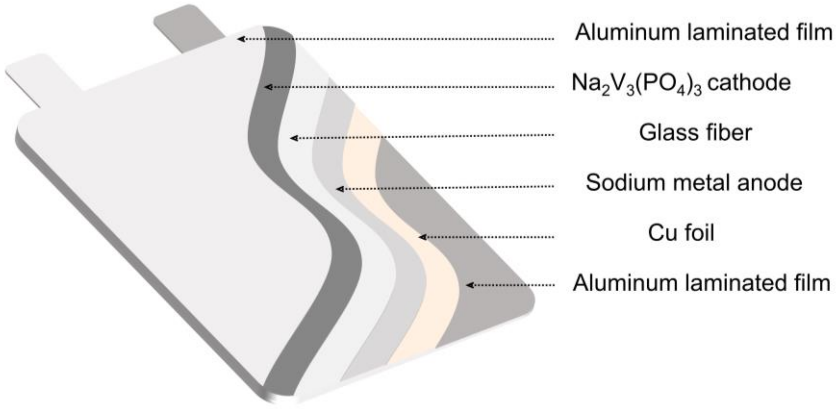

Figure S15. Structure of sodium metal pouch cells.

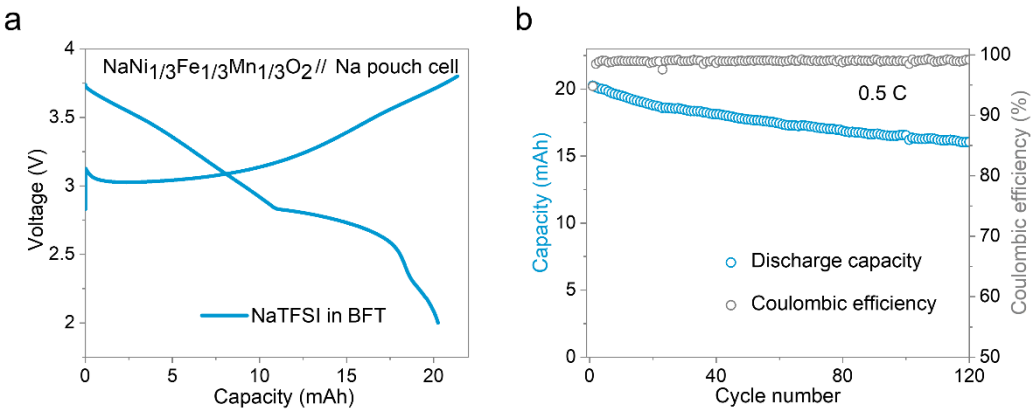

Figure S16. The electrochemical performance of $NaNi_{1/3}Fe_{1/3}Mn_{1/3}O_2$//Na pouch cells in NaTFSI in BFT electrolyte. (a) The first charge and discharge curves of $NaNi_{1/3}Fe_{1/3}Mn_{1/3}O_2$//Na pouch cell at 0.5 C between 2.0-3.8 V; (b) The cycling performance and coulombic efficiency for the $NaNi_{1/3}Fe_{1/3}Mn_{1/3}O_2$//Na pouch cell at 0.5 C between 2.0-3.8 V.

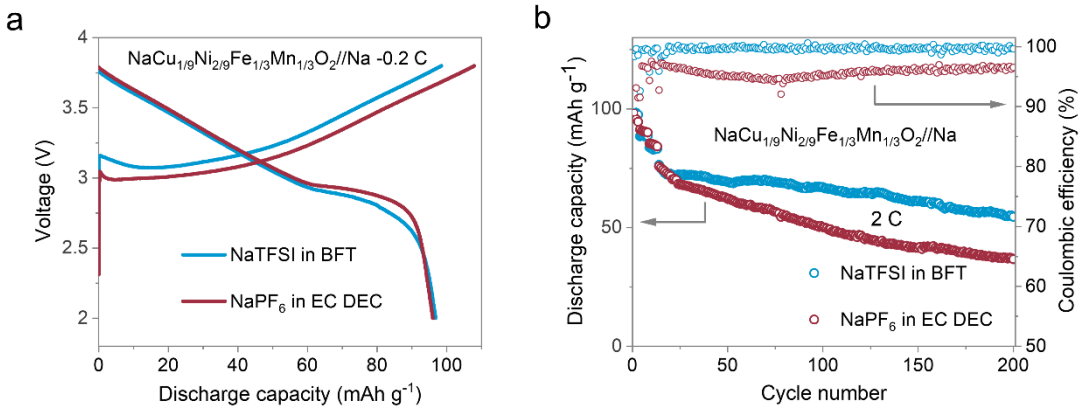

Figure S17. The electrochemical performance of $NaCu_{1/9}Ni_{2/9}Fe_{1/3}Mn_{1/3}O_2$//Na cells in NaTFSI in BFT and $NaPF_6$ in EC DEC electrolytes. (a) The first charge and discharge curves of $NaCu_{1/9}Ni_{2/9}Fe_{1/3}Mn_{1/3}O_2$//Na in NaTFSI in BFT and $NaPF_6$ in EC DEC electrolytes at 0.2 C between 2.0-3.8 V; (b) The cycling performance and coulombic efficiency of $NaCu_{1/9}Ni_{2/9}Fe_{1/3}Mn_{1/3}O_2$//Na in NaTFSI in BFT and $NaPF_6$ in EC DEC electrolytes between 2.0-3.8 V (3 cycles at 0.2 C, 5 cycles at 0.5 C, 5 cycles at 1 C and then keep cycling at 2 C).